euspen's 23rd International Conference & Exhibition, Copenhagen, DK, June 2023
www.euspen.eu

Force sensing linear rolling guides based on modified metal strain gauges

Berend Denkena[1], Heinrich Klemme[1], Dennis Kowalke[1*], Michael Korbacher[2], Rico Ottermann[3], Folke Dencker[3], Marc Christopher Wurz[3]

[1]*Institute of Production Engineering and Machine Tools (IFW), Hannover, Germany*
[2]*Bosch Rexroth AG, Schweinfurt, Germany*
[3]*Institute of Micro Production Technology (IMPT), Hannover, Germany*

** kowalke@ifw.uni-hannover.de*

Abstract
Monitoring machining processes can help to increase the quality of machined workpieces. However, not all relevant information (e.g. process forces) can be sufficiently obtained by observing the drive signals. Various sensory devices have been developed during the last years to overcome this deficit. Such sensory devices include spindle slides, clamping systems, and tool holders. These devices are usually exclusively designed for individual machines or processes. Thus, these systems can rarely be adapted for other use cases affecting their scope of application. Other sensor concepts reduce the stiffness of the machine tool and therefore the machining accuracy. As a standardized component in machine tools, linear guides offer the potential to measure forces without reducing the stiffness of the machine tool. Thus, this paper presents a novel approach for force measurement with sensory linear rolling guides. Compared to previous approaches, the number of sensors is reduced, decreasing manufacturing effort. Considering the high stiffness of the guide carriage and the resulting low strains, foil-based modified metal strain gauges with a gauge factor $k \approx 10$ are used to measure forces perpendicular to the guide rail. Based on an FE-simulation, adequate sensor positions are selected. A prototype of the sensory guide carriage is evaluated on a tensile test stand to determine the minimal measurable force based on the signal-to-noise ratio and the signal drift. The signals of the strain gauges allow a force resolution of 0.11 % of the load rating of the guide carriage. This is achieved by using a Kalman filter based state estimation model to compensate for the noise.

Strain gauge, force measurement, linear rolling guide, machine tools

1. Introduction

Advances in machine control and sensory equipment allow process monitoring for individual machining setups [1, 2]. Dynamometers and sensory tool holders are available to measure process forces. Due to high acquisition costs and setup efforts those systems are unsuitable for manufacturing with varying tools and workpiece geometries. Moreover, these additional components reduce the overall stiffness. For these reasons, structure-integrated sensors have been increasingly researched during the last years (e.g. [3-5]). Due to the unique design of the investigated components, however, the sensor concept needs to be developed for every machine type individually. Widely used and standardized components in machine tools and other industrial machines are linear rolling guides [6]. Due to their standardization, linear rolling guides offer great potential to integrate cost-efficient force measurement sensors for process monitoring.

Previous works have studied the suitability of the guide carriage to measure process forces. A guide carriage and its constituent parts are shown in Fig. 1a and Fig. 1b. Krampert et al. [7] investigated guide carriages under uniaxial load using multiple strain gauges between the steel inlays and the guide carriage. Four strain gauges on different sections of the guide carriages side faces were used by Denkena et al. [8] to measure two-axial forces with a non-moving guide carriage. The results showed a peak difference of 145 N between the measured and reference force.

Contrary to previous research, the underlying article investigates a two-axial force measurement using only two strain gauge sensors on the front face. Furthermore, this approach potentially allows for an automated sensor application as the application takes place on only one surface. The investigations are done using a Bosch Rexroth R18514 linear rolling guide carriage. At first, section 2 presents the sensory guide carriage regarding the sensor positioning and the applied strain gauges. Subsequently, section 3 presents the experimental evaluation of the sensory capabilities for each force direction using a tensile test stand. Finally, the calculation of forces from the experimental data is evaluated using a signal offset method (Section 4.1) and a Kalman filter enhancing the offset method (Section 4.2).

2. Sensory guide carriage and sensor positions

Typically, a significant proportion of the front face of a sensory guide carriage is covered by end caps, as shown in Fig. 1b. The end caps seal the guide against pollution as it is part of the lubrication system. The end caps are also a vital part of the roller recirculation system. Higher strains occur due to structurally weakened stiffness between the inside corners and the recirculation bores. This can be seen in Fig. 1d for a load of 100 N in the Y-direction and in Fig. 1e for 100 N in the Z-direction. The simulations use a simplified model of the carriage. To allow the manual application of the strain gauges with adhesive without restricting the function of the guide system, one end cap is modified to separate the strain gauges and their electrical wiring (not illustrated) from the lubrication area. The area between the inside corner for the profile rail, the recirculation bore, and a thread hole for screwing the end cap is most suitable for applying the strain gauges. The application at this position offers a compromise regarding high strain amplitudes, a large surface area, and good accessibility. To ensure high sensitivity while reducing possible thermal effects, modified metal strain gauges of type 1-3-SD-VB-08-01.25-01.XX from CeLaGo Sensors were used. The strain gauges are made from carbon doped with NiCr and have a gauge factor of $k_{mod} \approx 10$ [9]. Therefore, they are approximately five times more sensitive than regular metal strain gauges made from constantan with $k_{co} \approx 2$. The first sensor and the position of the second sensor (not yet attached in Fig. 1) are shown in Fig. 1a. The sensors are designed as full bridges on a polyimide carrier film with a surface area of A_{SG} = 5 mm x 5 mm to reduce interactions between the strain gauges and the mounted end cap and to allow for the sealing of the lubrication area. One applied sensor is shown in Fig. 1c. The suitable orientations of the strain gauges were determined based on FE simulations of the main vector of the elastic strain (Fig. 1d/e). The simulated strain at the identified positions is $\varepsilon_Y \approx 0.4$ µm/m for a force of 100 N in the Y-direction and $\varepsilon_Z \approx 0.16$ µm/m for a force of 100 N in the Z-direction. Thus, the expected strain is about four times higher compared to the side face strains determined in [8].

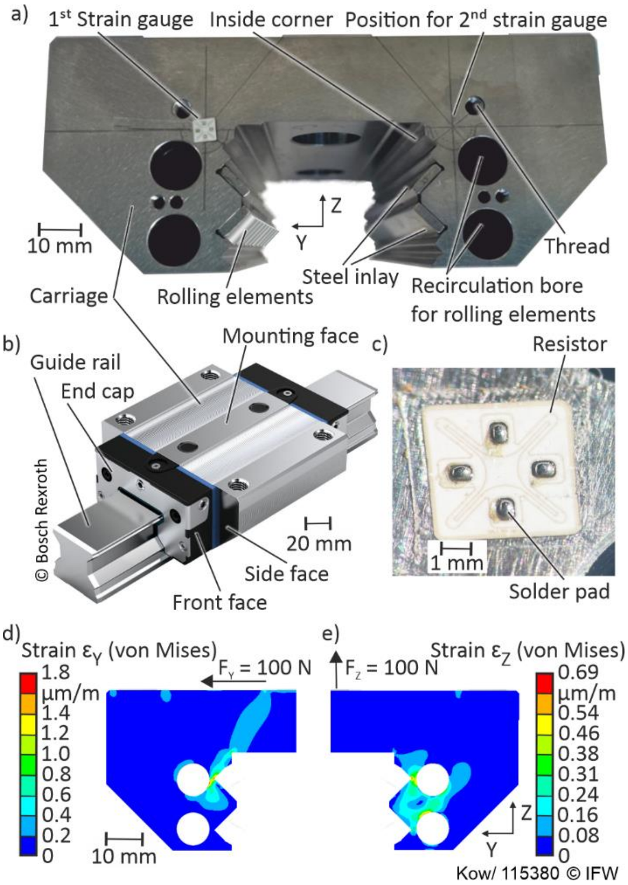

Figure 1. Position (a) of the strain gauges (c) on a linear rolling guide (b) and the simulated strains for loads in Y- (d) and Z-direction (e)

3. Experimental evaluation

To evaluate the sensory guide carriage, a tensile test stand (Mecmesin MultiTest 2,5-xt) is used to apply defined forces to the guide system (Fig. 2a). The test stand and the guide carriage are connected through an adapter. The adapter can be set up for either force application in the Z-direction (Fig. 2b) or Y-direction (Fig. 2c). A dynamometer (Kistler 9257B) is integrated to measure the reference forces (F_Y and F_Z) applied to the guide carriage. The force and strain gauge signals are digitized at 1000 Hz using Beckhoff EtherCAT analog input Terminals (EL3104, EL3356) in combination with a Beckhoff industrial PC.

Table 1 Test parameters

Experiment	Load level		Test direction
	F_{min}	F_{max}	
1	400 N	500 N	Z
2	-400 N	-450 N	Y
3	-400 N	-425 N	Y
4	-400 N	-415 N	Y

The maximum deviation between the reconstructed force from the strain gauge signals and the reference force from the dynamometer is evaluated using different load levels. The values for the load levels (F_{min} and F_{max}) are shown in Table 1. Each experiment consists of three repetitions of two load levels. The force of each load level was held constant for 2 s.

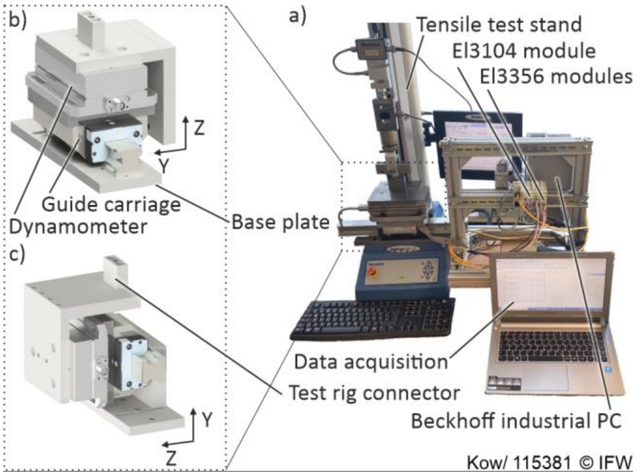

Figure 2. Tensile test stand (a) for testing in Z- (b) and Y-direction (c)

The data obtained from experiment 1 with the test parameters stated in Table 1 is shown in Fig. 3. The graph shows the measured force and normalized sensor signals from both strain gauges SG_1 and SG_2. The graph indicates a clear correlation between both sensor signals and the force signal. Therefore, the signals are suitable for directly calculating the force in Z-direction. The signals of SG_2 have an approximately ten times higher noise amplitude than the signals of SG_1. Investigations showed that one EL3356 Terminals added noise to the digitized signal. Both strain gauges have similar signal amplitudes. The course of SG_1 starts to drift towards lower signals after t = 39 s. Possible causes for the drift are changes in the light incidence that only affected SG_1.

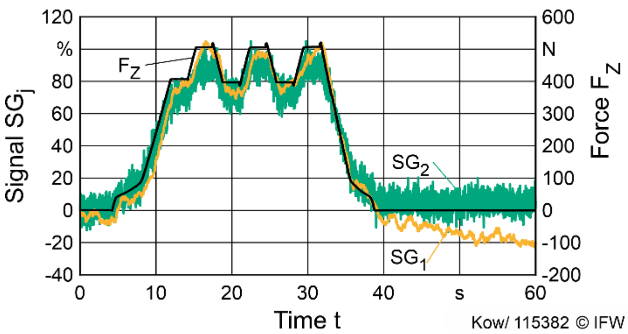

Figure 3. Raw signals for testing in Z-direction

Using the setup for applying force in the Y-direction and the parameters for experiment 2 the data shown in Fig. 4 was obtained. Assuming a normally distributed noise, the standard deviation was calculated. During a period without load (t ≤ 10 s), standard deviations corresponding to a force of 3.6 N for SG_1, 12.57 N for SG_2, and 1.8 N for F_Y are obtained. During the last load (450 N; 39.5 s < t ≤ 40.5 s), standard deviations of 3.8 N for SG_1, 15.2 N for SG_2, and 1.0 N for F_Y are obtained. It shows that the strain gauge signal SG_1 has a positive correlation with the force signal F_Y whereas the SG_2 has a negative correlation. Therefore, no proportional correlation between the sensor signals and the forces can be used to reconstruct the forces directly. As the forces cannot be calculated directly when a force in the Y-direction is present, substitute values are necessary.

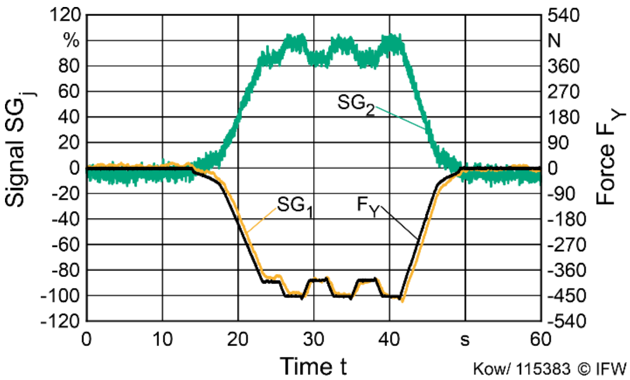

Figure 4. Raw signals for testing in Y-direction

4. Force reconstruction

Two methods are considered to reconstruct the force signals for Y- and Z-direction from the strain gauge signals. First, the force is reconstructed using the sum and difference of the strain gauge signals (Section 4.1). In section 4.2 a Kalman filter [10] is used. Finally, the results of both methods are compared.

4.1. Force reconstruction with an offset signal

Substitute values for the force reconstruction are the sum of the strain gauge signals $S_{offset;sum}$ and their difference $S_{offset;diff}$ as stated in Eq. 4-1 and Eq. 4-2

$$S_{offset;sum} = SG_1 + SG_2 \qquad (4\text{-}1)$$

$$S_{offset;diff} = SG_1 - SG_2 \qquad (4\text{-}2)$$

The calculated substitute values for experiment 2 are presented in Fig. 5a. The deviation between the calculated signal and the corresponding forces in Z- and Y-direction is displayed in Fig. 5b. The deviation is calculated using the normalized force signals F_Y and F_Z. The graph shows that the deviation remains within a range of ± 10 %. Therefore, the deviation interval is 90 N. The calculated standard deviations for the Z-direction are 12.7 N (no load; t ≤ 10 s) and 14.8 N (load of 450 N; 39.5 s < t ≤ 40.5 s). For the Y-direction the calculated standard deviations are 13.4 N (t ≤ 10 s) and 16.6 N (39.5 s < t ≤ 40.5 s).

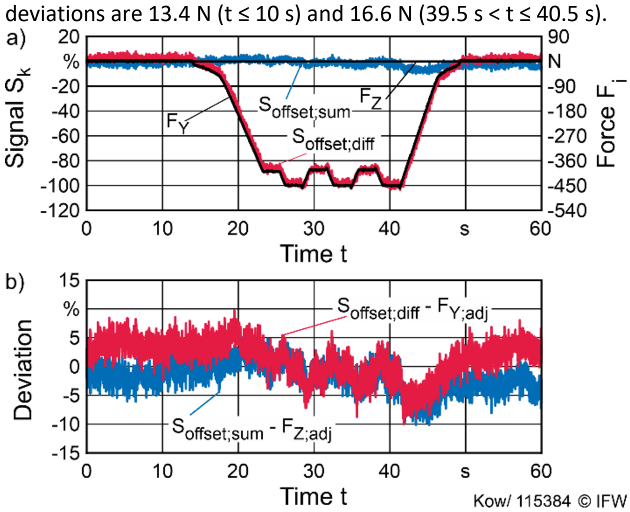

Figure 5. Processed signals for testing in Y-direction

4.2. Force reconstruction with Kalman filter

The offset method is transferred into a Kalman filter to reduce the deviation between the reference force signals and the reconstructed signals. The deviation is evaluated using the deviation interval to consider the maximum deviation and the mean sum of all squared deviations to consider the average deviation. The guide carriage is modeled with the state space x_k. The state space consists of four states and describes the guide carriage at each time t_k. The first two states represent the last strain gauges signal values. The third state represents the force in the Y-direction and is given as K_{diff}. The fourth state represents the force in the Z-direction and is given as K_{sum}. The actual signal values of the strain gauges are used as the observation z_k. The state-transition model F_k describes the influence of the last state x_{k-1} resulting in the new estimation $x_{k|k-1}$ (Eq. 4-3).

$$x_{k|k-1} = F_k x_{k-1} \qquad (4\text{-}3)$$

The a-priori covariance matrix for the estimation $x_{k|k-1}$ is described by $P_{k|k-1}$. It is calculated according to Eq. 4-4.

$$P_{k|k-1} = F_{k-1}P_{k-1}F_{k-1}^T + Q_{k-1} \qquad (4\text{-}4)$$

The calculations of $x_{k|k-1}$ and $P_{k|k-1}$ predict the new state for the current step. After that, the prediction is corrected using the current signal value and information about the uncertainty. The Kalman gain K_k is calculated as indicated in Eq. 4-5. The Kalman gain represents the responsiveness between input changes and their influence on the state space x_k.

$$K_k = P_{k|k-1}H_k^T(H_k P_{k|k-1}H_k^T + R_k)^{-1} \qquad (4\text{-}5)$$

The Kalman gain is used as a factor for the divergence between the actual signal value z_k and the expected value. The expected reading is the product of the observation model and the estimated state. This divergence term is added to the estimated state $x_{k|k-1}$ to correct the prediction as Eq. 4-6 states.

$$x_k = x_{k|k-1} + K_k(z_k - H_k x_{k|k-1}) \qquad (4\text{-}6)$$

The a-posteriori covariance matrix for x_k is described by P_k.

$$P_k = (I - K_k H_k)P_{k|k-1} \qquad (4\text{-}7)$$

The system is described by the state-transition model (Eq. 4-8).

$$F_k = \begin{pmatrix} 1 & 0 & 0 & 0 \\ 0 & 1 & 0 & 0 \\ a & -a & 1-a & 0 \\ a & a & 0 & 1-a \end{pmatrix} \qquad (4\text{-}8)$$

The observation model H_k describes the correlation between the systems states and the observation made (Eq. 4-9).

$$H_k = \begin{pmatrix} 1 & 0 & 0 & 0 \\ 0 & 1 & 0 & 0 \end{pmatrix} \qquad (4\text{-}9)$$

Assumptions about the initial system state and the related covariance are needed. For the initial state, it is assumed that all states are zero. Its initial covariance is assumed using Eq. 4-10.

$$P_{0|init} = \begin{pmatrix} \sigma^2 & 0 \\ 0 & \sigma^2 \end{pmatrix} \qquad (4\text{-}10)$$

For the observation and process noise covariance $R_k = 5 \cdot I_2$ and $Q_k = 30 \cdot I_4$ are estimated, with I_2 and I_4 being unit matrices with rank 2, respectively 4. With a = 0.24, the parameter for F_k is optimized, so the mean sum of all squared deviations is lower for the Kalman filter than the offset signal. Before applying load (0 N; t ≤ 10 s) the standard deviations are 3.9 N for Y-direction and 3.3 N for Z-direction. During load (450 N; 39.5 s < t ≤ 40.5 s) the standard deviations are 4.7 N for Y-direction and 3.0 N for Z-direction. The optimized data is plotted, as well as the reference forces and the offset signals in Fig. 6a. The deviation between the Kalman-filtered signals and the offset signals are shown in Fig. 6b for the Z-direction and in Fig. 6c for the Y-direction.

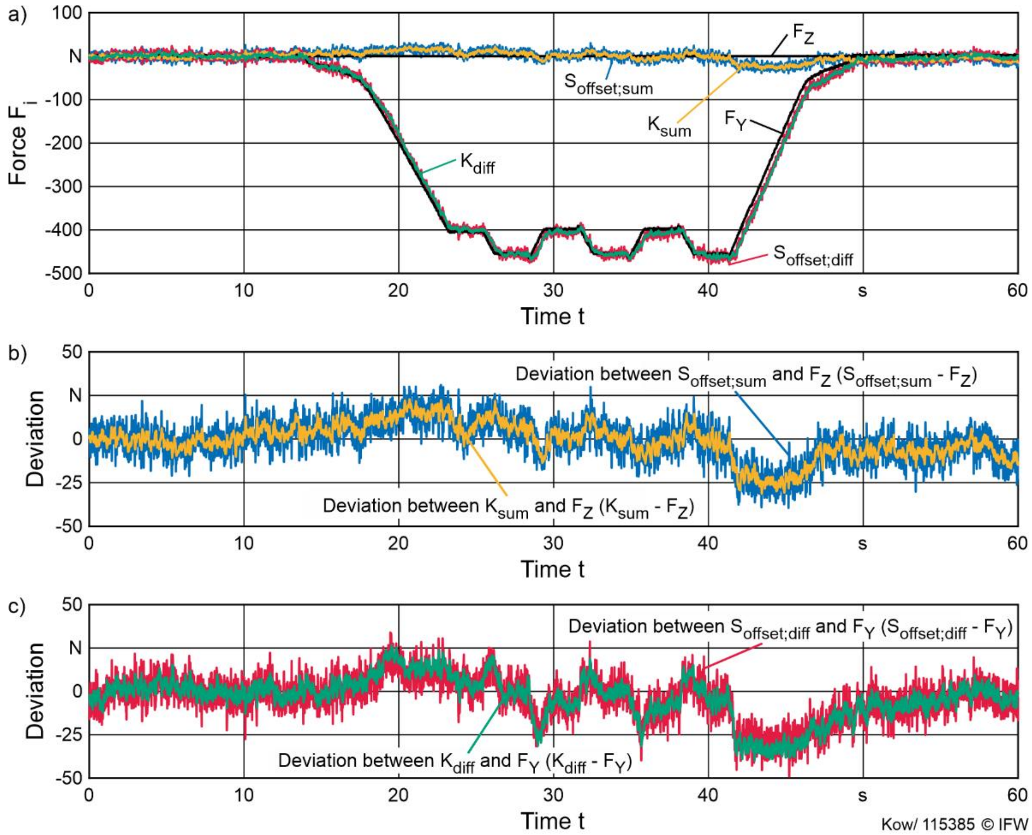

Figure 6. Kalman-filtered signals for testing in Y-direction

For the Z-direction, the Kalman-filtered signal has a deviation between -31 N and 23 N, while the offset signal has a deviation between -39 N and 31 N. For the Y-direction, the Kalman-filtered signal has a deviation between -40 N and 27 N, compared to -49 N and 34 N for the offset signal. For the Kalman-filtered signal, the deviation in the Z-direction remains within an interval of 54 N and remains within an interval of 67 N for the Y-direction. Compared to the offset signals, the deviation is about 20 % lower. The data from experiments 3 and 4 show comparable courses and values for the deviation. The deviation peaks coincide with the load changes in terms of time and direction. The total deviation interval is 121 N. Compared to the dynamic load rating of the carriage (C = 106.6 kN), this is 0.11 %.

5. Summary and conclusion

This paper shows a novel approach for equipping linear roller guides with strain gauges to sense forces in two directions. To increase the sensitivity compared to previous research, the front face of the guide carriage was considered for identifying suitable sensor positions. A guide carriage was equipped with two modified metal strain gauges and evaluated on a tensile test stand. Two methods for reconstructing the applied forces from the strain gauge signals were compared using measurement data. The first method calculates substitute values that are force proportional by offsetting one strain gauge signal against the normal and inverted signal of the second strain gauge. For the second method, the first method is extended with a Kalman filter. The Kalman filter reduced the deviation by 20 %. A deviation of 66 N for the Y-direction and 52 N for the Z-direction was achieved. Compared to [8], with an achieved deviation of 145 N at a reference force of -500 N in the Z-direction, the deviation using the Kalman filter is less than 50 %.

Further research should consider the sensor behavior during the motion of the guide carriage. Therefore, the state-transition model needs to be improved to include the velocity and position of the guide carriage. Moreover, it is necessary to extend the experiments to higher loads to investigate for effects during preload release and possible influences toward linearity at higher loads. Using directly deposited strain gauges [11] could additionally increase the signal quality due to the missing polyamide carrier film between the guide carriage material and the sensor material. Additionally, the use of directly deposited sensors in combination with a sensitivity analysis should lead to a higher sensitivity due to a more precise sensor positioning and the possibility of individualizing the sensor structures. Studies are currently being conducted on this.

Acknowledgment

The authors thank the German Research Foundation (Deutsche Forschungsgemeinschaft – DFG), which funded this work within the research project “Force-sensitive Guide Systems Based on Directly Deposited Component-Specific Sensors” - 428561441.

References

[1] Denkena B, Dahlmann D, Kiesner J 2016 *Procedia Tech.* **26** 235-244

[2] Möhring H C, Litwinski K M, Gümmer O 2010 *CIRP Annals* **59(1)** 383-386

[3] Brecher C, Klatte M, Wenzel C 2015 *Laser Metrology and Machine Perpormance* **XI**

[4] Möhring H C, Wiederkehr P, Lerez C, Schmitz H, Goldau H, Czichy C 2016 *Procedia Tech.* **26** 120-128

[5] Denkena B, Boujnah H 2018 *CIRP Annals* **67(1)** 423-426

[6] Bosch Rexroth AG 2007 Linear Motion Technology Handbook Schweinfurt Bosch

[7] Krampert D, Unsleber S, Jannsen C, Reindl L 2019 *Sensors* **19** 3411

[8] Denkena B, Park J K, Bergmann B, Schreiber P 2018 *euspen's 18th International Conference & Exhibition* 123-124

[9] CeLaGo Sensors GmbH 2022 Data sheet – Strain gauge https://www.celago-sensors.de/app/download/17462624296/Data+sheet_SD_V1.20e.pdf?t=1652861000

[10] Kalman R E 1960 *Transactions of the ASME--Journal of Basic Engineering* **82** 35-45

[11] Ottermann R, Zhang S, Denkena B, Klemme H, Kowalke D, Korbacher M, Dencker F, Wurz M C 2022 *IEEE Sensors* 1-4